

Phase Behavior and Thermodynamic Phenomena of Hyperbranched Polymer Solutions

Matthias Seiler, Jörn Rolker, and Wolfgang Arlt*

Fachgebiet Thermodynamik und Thermische Verfahrenstechnik, Institut fuer Verfahrenstechnik, Sekr. TK 7, Technical University of Berlin, Strasse des 17. Juni 135, D-10623 Berlin, Germany

Received December 20, 2002

ABSTRACT: The understanding of the phase behavior of dendritic polymers, i.e., hyperbranched polymers and dendrimers, is still in its infancy. No systematic thermodynamic investigations on the phase behavior of dendritic polymer solutions have been reported so far. Therefore, this experimental study focuses on the low- and high-pressure phase behavior of hyperbranched polymer–solvent and hyperbranched polymer–solvent–supercritical gas systems. The influence of the solvent polarity, the nature and number of polymer functionalities, and the degree of polymer branching, as well as the polymer and supercritical gas concentration on the phase behavior of selected hyperbranched polymer solutions, is discussed. Thermodynamic phenomena such as the merging of the upper critical solution temperature (UCST) and the lower critical solution temperature (LCST) curves, the pH dependence of the polymer solubility and a remarkably distinct solutropic phase behavior are presented.

1. Introduction

Hyperbranched polymers represent highly branched, polydisperse macromolecules with a treelike topology and a large number of functional groups. These kinds of polymer structures are known from polysaccharides such as glycogen, dextran, and amylopectin since the 1930s.¹ In 1952, Flory discussed the synthesis of branched condensation polymers by step-growth polymerization from multifunctional monomers.² However, since he expected highly branched, nonentangled polymers with a broad molecular weight distribution and poor mechanical properties, he did not pursue this synthetic methodology further. During the last 10 years, the rapidly growing interdisciplinary interest in the structurally perfect dendrimers promoted the rediscovery of hyperbranched polymers.³ The tedious and complex multistep synthesis of dendrimers results in expensive products with limited use for large-scale industrial applications. For many applications, which do not require structural perfection, using hyperbranched polymers can circumvent this major drawback of dendrimers. Unlike dendrimers, randomly branched hyperbranched polymers with similar properties can be easily synthesized via one-step reactions and therefore also represent economically promising products for large-scale industrial applications. Companies such as the Perstorp Group (Perstorp, Sweden) and DSM Fine Chemicals (Geleen, Netherlands) already produce commercially available hyperbranched polymers on a large scale.⁴⁰ Most of the applications of hyperbranched polymers are based on the absence of chain entanglements and the nature and the large number of functional groups within a molecule. The functionalities of hyperbranched polymers allow for the tailoring of their chemical, thermal, rheological, and solution properties and thus provide a powerful tool to design hyperbranched polymers for a wide variety of applications.³

An area of application that, until now, has remained unconsidered in scientific discussions is the field of

process engineering. Since the polarity of hyperbranched macromolecules can be adjusted by controlled functionalization of the end groups, selective solvents (consisting of either pure hyperbranched polymers or fractions of hyperbranched additives) can be tailored.³ Unlike the conventional linear polymers, hyperbranched polymers show not only a remarkable selectivity and capacity⁴ but, in many cases, also a comparatively lower solution and melt viscosity⁵ as well as an enormous thermal stability.⁶ Therefore, hyperbranched polymers can be used for optimizing a number of separation and production processes. Even a variety of biomedical applications seems possible.^{7,8} Only recently, the authors suggested the use of hyperbranched polymers as entrainers for extractive distillation^{3,4,9,10} and as selective solvents for liquid–liquid extraction.^{4,10} Figure 1 illustrates the breaking of the tetrahydrofuran–water and the ethanol–water azeotropes by adding commercially available, highly selective hyperbranched polymers to the azeotropic systems. In Figure 2, a remarkably distinct solutropic phenomenon is depicted for the ternary system tetrahydrofuran–water–hyperbranched polyester. The broad liquid–liquid miscibility gap allows for the breaking of the tetrahydrofuran–water azeotrope by means of solvent extraction.⁴ Furthermore, also the use of hyperbranched polymers as selectivity- and capacity-increasing solvent additives for absorption processes and as stationary phases for preparative chromatography seems promising.¹¹

The large body of interdisciplinary research on dendritic polymers, i.e., dendrimers and hyperbranched polymers, is a guarantee for emerging applications.^{3,12–14} However, the understanding of essential fundamentals such as the phase behavior of dendritic polymer solutions is still in its infancy. The experimental investigation of the phase behavior of hyperbranched polymer systems is a crucial requirement for a successful introduction of new applications to highly competitive markets. In this context, thermodynamic models, which accurately account for the impact of polymer branching on the phase behavior of polymer systems, play a very important role; they enable the optimization of new

* Corresponding author. Tel.: ++49–30–31423977; fax: ++49–30–31422406. E-mail: W.Arlt@vt.tu-berlin.de.

Table 1. Polymer Samples Used

sample	molar mass (g/mol)	M_w/M_n	no. of OH groups per macromolecule	hydroxyl no. (mg KOH/g)	acid no. (mg KOH/g)	provider
Hybrane H1500	$M_n = 1500$	≈ 5	8			DSM
Boltorn H20	$M_w = 2100$	1.3	16	490–520	5–9	Perstorp
Boltorn H40	$M_w = 5100$	1.8	64	470–500	7–11	Perstorp

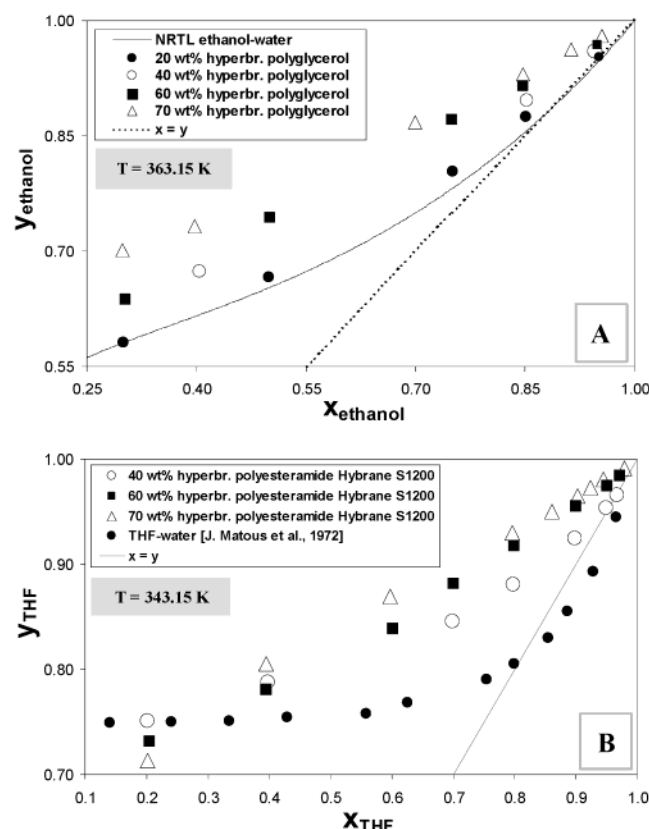


Figure 1. Influence of hyperbranched polymers on vapor-liquid equilibria of aqueous azeotropic systems:^{9,38} (A) ethanol-water-hyperbranched polyglycerol at 363.15 K;⁹ (B) THF-water-hyperbranched polyesteramide Hybrane S1200 at 343.15 K.³⁸

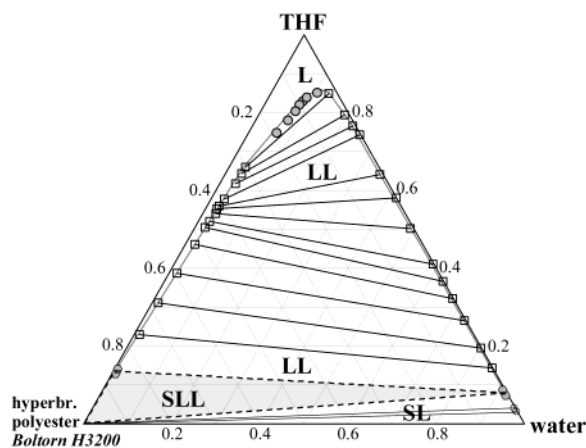


Figure 2. Experimental liquid-liquid (LLE), solid-liquid-liquid (SLLE), and solid-liquid (SLE) equilibrium results of the ternary system THF-water-hyperbranched polyester at $T_{\text{equilibrium}} = 321.15 \text{ K}$.⁴

applications of hyperbranched polymers without requiring an unjustifiable amount of experimental phase equilibrium data. But so far, despite the scientific effort of thermodynamicists in this field,³ no g^E -model or equation of state has been developed, which proved to be suitable

in considering explicitly the influence of the degree of polymer branching on the phase behavior of highly branched polymer systems over a wide temperature and pressure range. An important prerequisite for the development and testing of new thermodynamic models is the availability of appropriate experimental phase equilibrium data, especially in the high-pressure range. But until now, no experimental studies on the high-pressure phase behavior of dendritic polymer systems have been carried out.

Therefore, this paper aims at providing the first extensive experimental study on the phase behavior of hyperbranched polymer-solvent and hyperbranched polymer-solvent-supercritical gas systems. Both the phase behavior at moderate and at high pressure are investigated systematically. The influence of the nature and number of polymer functionalities, the degree of polymer branching, and the solvent polarity as well as the concentration of a supercritical gas on the phase behavior of selected hyperbranched polymer solutions is discussed.⁴¹

2. Experimental Section

2.1. Apparatus and Experimental Procedure. 2.1.1.

Gravimetric Method. Vapor-liquid equilibria of polymer-solvent systems at 393.15 K were measured using a gravimetric-sorption method. The experimental apparatus and the experimental procedure are accurately described by Sadowski et al.¹⁵

2.1.2. Cloud-Point Measurements. Upper and lower solution temperature curves as well as the LLV curve of hyperbranched polyester solutions were determined using a variable-volume autoclave of about 1 dm³ designed for liquid-liquid (LL), vapor-liquid-liquid (VLL), and vapor-liquid-solid (VLS) experiments at pressures up to 20 MPa and temperatures up to 520 K. A detailed description of the autoclave has been given earlier.^{16,17} The experimental procedure has been previously described by several authors, e.g. Bungert et al.¹⁷ and Chen et al.¹⁸

2.2 Materials. Perstorp Speciality Chemicals AB provided aliphatic hyperbranched polyesters, known as the Boltorn family. The Boltorn samples used (*Boltorn H20* and *Boltorn H40*) are hydroxyl functional hyperbranched polyesters, which are produced from polyalcohol cores and hydroxy acids. DSM provided the hyperbranched polyesteramide *Hybrane H1500*. The specifications of the hyperbranched polymers used are listed in Table 1. Ethanol (purity > 99.8 mol %) was obtained from Merck and carbon dioxide (technical grade, purity > 99.5 mol %) was provided by Linde. Both ethanol and carbon dioxide were used as received. Distilled water was degassed and repeatedly filtered using a 0.2 μm Millipore filter in order to remove dust.

3. Results and Discussion

The following experimental results describe the phase behavior of hyperbranched polymer solutions over a wide pressure and temperature range. For a better understanding, the qualitative arrangement of the investigated miscibility gaps is illustrated in Figure 3.

Figure 3A schematically shows the phase behavior of a binary monodisperse polymer-solvent system with an upper critical solution temperature (UCST). At low

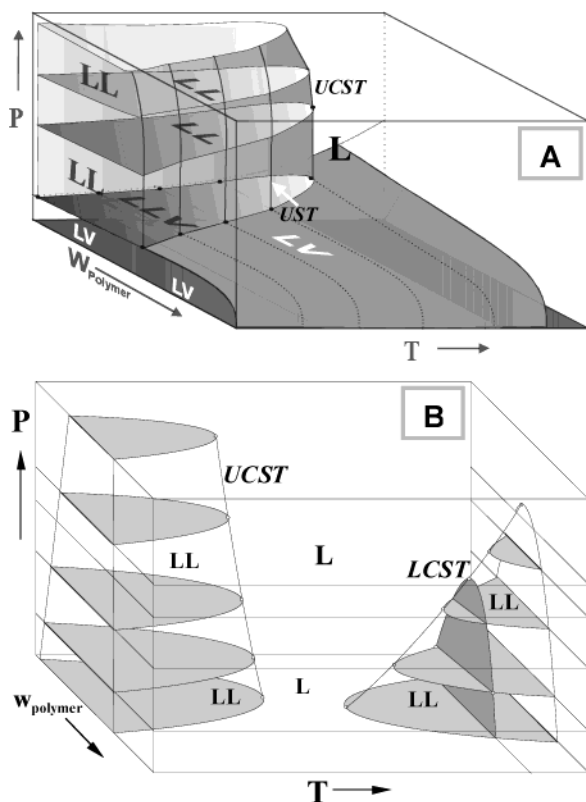


Figure 3. Qualitative arrangement of the investigated miscibility gaps of hyperbranched polymer solutions at moderate and high pressures: (A) low- and high-pressure phase behavior in the vicinity of the upper critical solution temperature; (B) high-pressure phase behavior showing an upper critical and a lower critical miscibility gap.

pressure, the vapor–liquid equilibrium (VLE) can be found, which—for a limited polymer concentration range and pressures larger than the vapor pressure of the solvent—is superposed by a liquid–liquid miscibility gap. At moderate temperatures, the UCST curve separates this miscibility gap from the homogeneous polymer solution. Upon heating, due to thermal motions, the polymer solubility increases, resulting in the disappearance of the second liquid phase at $T > T_{UCST}$ (Figure 3B). When the temperature of the homogeneous system increases further, the solvent expands at a much faster rate than the polymer, leading to a continuous decrease in solvent power and the occurrence of a second liquid–liquid miscibility gap of LCST character at high temperatures. For further details see ref 3.

3.1. Phase Behavior at Moderate Pressure. 3.1.1.

Vapor–Liquid Equilibria. In Figure 4A, bubble point lines for different hyperbranched polymer–solvent systems are shown at an equilibrium temperature of 393.15 K (see also Table 2). In the case of ethanol as solvent, a steep rise of the isothermal partial pressure curves can be observed, whereas the lower solvent volatility of water results in a flatter curve shape. Although a variety of different hyperbranched polymer systems have been investigated, it becomes obvious that the different VLE are more dominated by the solvent volatility and polarity than by the structures of the respective hyperbranched polymer. It is known that the degree of branching has a pronounced effect on the radius of gyration and the center of mass diffusion of a polymer.¹⁹ However, when comparing polymers with a different degree of branching in the same solvent, only a small influence on the VLE was found such as

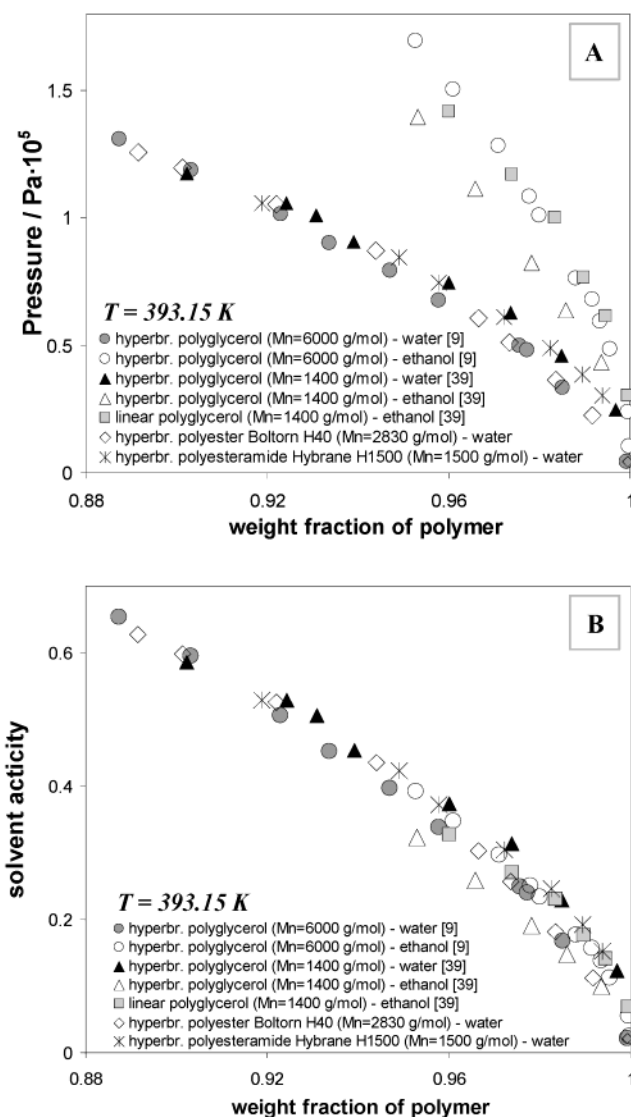


Figure 4. Vapor–liquid equilibria of different hyperbranched polymer–solvent systems at $T_{\text{equilibrium}} = 393.15$ K: (A) isothermal partial pressure curves of ethanol or water in different hyperbranched polymers; (B) solvent activity vs polymer weight fraction.

observed for the hyperbranched polyglycerol ($M_n = 1400$ g/mol) and its perfect linear polyglycerol analogue⁴² in ethanol. The ethanol absorption by polyglycerol tends to increase with decreasing molecular weight and increasing degree of polymer branching (Figure 4A). This corresponds to a comparatively lower ethanol activity in the hyperbranched polyglycerol ($M_n = 1400$ g/mol) solution (see Figure 4B).

Apart from the latter system, Figure 4B shows that there is almost no difference in the solvent activity for the investigated polymer solutions. This result underlines that the macromolecular topology, the chemical backbone structure, and, for a certain range, the molecular weight of the polymer are of minor importance for the VLE. When comparing the results of Figure 4, parts A and B with other VLE investigations,^{9,20,21} it can be concluded that the VLE of hyperbranched polymer solutions primarily depends on the interactions between the solvent molecules and the polymer functionalities.

3.1.2. Vapor–Liquid–Liquid Equilibria. In Figure 5, the bubble point curve (Figure 5A) and the

Table 2. VLE and LLV Results of Different Hyperbranched Polymer–Solvent Systems^a

Hybrane H1500–water VLE at $T = 393.15$ K		Boltorn H40–water			
		VLE at $T = 393.15$ K		LLV curve	
w_{polymer}	P (Pa)	w_{polymer}	P (Pa)	w_{polymer}	T (K)
0.919	105 770	0.817	144 340	0.062	364.4
0.949	84 500	0.891	125 640	0.082	378.1
0.958	74 535	0.901	119 650	0.100	412.2
0.972	61 025	0.922	105 200	0.130	414.4
0.983	49 210	0.944	87 080	0.170	406.0
0.989	38 420	0.967	60 560	0.201	394.1
0.994	30 400	0.972	51 270	0.300	377.5 ^c
		0.984	36 310	0.350	358.8 ^c
		0.992	22 350	0.398	331.6 ^c
		0.999	4 280		

^a Cooling/heating rate of LLV cloud point experiments ≈ 1 K/h, ^b Phase transition LLV \Rightarrow LV. ^c Phase transition LV \Rightarrow LLV.

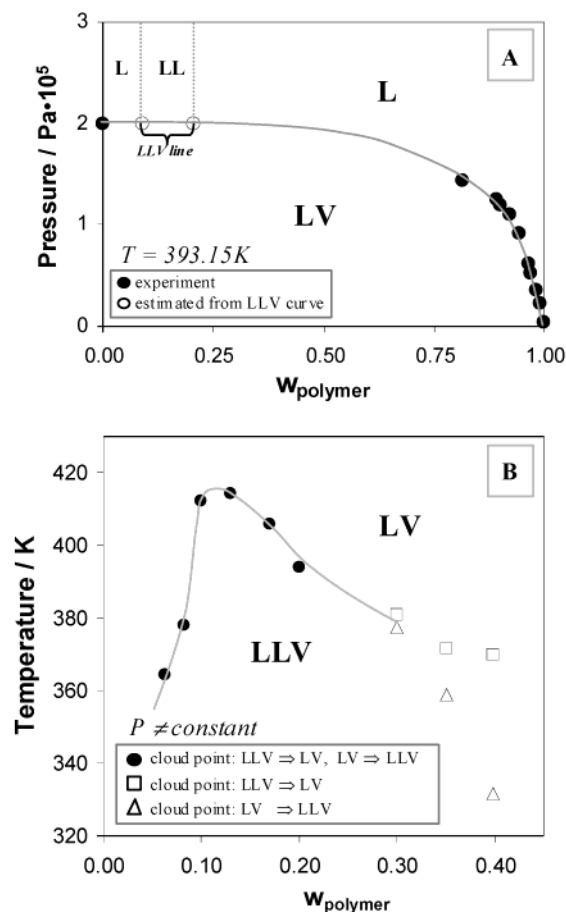


Figure 5. LLV and VLE results of the hyperbranched polyester solution Boltorn H40–water: (A) LLV curve in the pressure–concentration diagram as connection between the liquid–liquid miscibility gap (UCST-type) and the VLE; (B) LLV curve in the temperature–concentration space.

LLV curve (Figure 5B, Table 2) of the system water–hyperbranched aliphatic polyester Boltorn H40 are depicted. In addition to Figure 4, Figure 5A shows a part of the LLV–region at 393.15 K, i.e., the plateau upon which the UCST miscibility gap is located (see also Figure 3A). Experimental results for the LLV curve are illustrated in Figure 5B. At polymer concentrations < 30 wt %, the cloud point temperatures of the cooling procedure (LV \rightarrow LLV) coincide with the cloud point temperatures of the respective heating procedure (LLV \rightarrow LV). For the aqueous Boltorn H40 solutions with $w_{\text{polymer}} \geq 30$ wt %, the cloud point temperatures of the heating and cooling procedures show a deviation which increases with the polymer concentration. As observed

by Min Xu et al., due to their strong intermolecular interactions, hydroxyl-terminated hyperbranched aliphatic polyesters tend to form clusters in solution.²³ Particularly at high polymer concentrations, the macromolecular agglomerate formation is likely. Therefore, we presume that the deviations of the cloud point measurements at large polymer concentrations are due to hydrogen-bonded hyperbranched polymer clusters, which require more energy for their dissolution.^{24,25} Thus, the heating induced phase transition (LLV \rightarrow LV) is located at higher temperatures than the cooling induced demixing temperature (LV \rightarrow LLV). Further investigations on the nucleation and growth mechanism as well as on the spinodal decomposition mechanism will lead to a better understanding of the underlying phenomena.²⁵

3.2. High-Pressure Phase Behavior. The following high-pressure phase equilibria focus on the UCST and LCST miscibility gaps of hyperbranched polyester–solvent and hyperbranched polyester–solvent–CO₂ systems. Because of the concentration dependence of UCST and LCST curves, the chosen polymer–solvent weight fraction of $w_{\text{polymer}} = 0.10$ (on a gas free basis) does not always coincide with the critical concentration of the respective miscibility gap. Therefore, in the following, the presented miscibility curves will be termed upper and lower solution temperature (UST and LST) curves.

3.2.1. Hyperbranched Polyester–Water–CO₂. Figure 6 displays UST curves of aqueous hyperbranched polymer solutions. As polymers, two hyperbranched polyesters of different generations, Boltorn H20 and Boltorn H40, were used. When comparing the two CO₂-free polymer solutions ($w_{\text{polymer}} = 0.10$, see circles), the influence of the molecular Boltorn weight on the polymer solubility becomes evident. Despite the larger number of hydroxyl groups, the bigger Boltorn H40 molecules (4 pseudo-generations) are less soluble in water than the smaller hyperbranched polyester Boltorn H20 (2 pseudo-generations). Hence, the UST curve of the CO₂-free Boltorn H20 system is located approximately 45 K lower than the one of the Boltorn H40 solution.

As Figure 6 (triangles, squares) shows, the addition of CO₂ to the respective aqueous polyester solution of $w_{\text{polymer}} = 0.10$ shifts the UST curve to lower temperatures (see also Tables 3 and 4). For both gas-containing hyperbranched polyester solutions, this temperature shift corresponds to an increased polymer solubility.

When discussing the influence of the CO₂ concentration on the UST-location of hyperbranched polymer

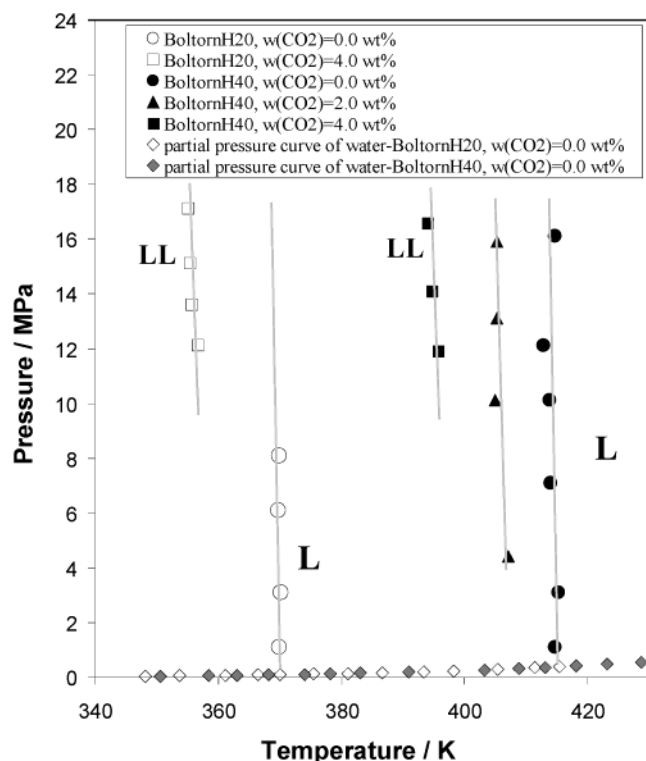


Figure 6. Influence of the CO₂ concentration on the location of the upper solution temperature curve for two aqueous hyperbranched polyester solutions containing polymers of different molecular weight (Boltorn H20 and Boltorn H40).

Table 3. UST Results of Hyperbranched Polyester–Solvent–CO₂ Systems^a

<i>w</i> _{CO₂}	<i>P</i> (MPa)	<i>T</i> (K)
Boltorn H20–Water–CO ₂		
0.0	1.10	369.9
0.0	3.10	370.2
0.0	6.10	369.8
0.0	8.10	369.9
0.04	12.10	356.7
0.04	13.60	355.7
0.04	15.10	355.5
0.04	17.10	355.1
Boltorn H40–Water–CO ₂		
0.0	1.10	414.7
0.0	3.10	415.0
0.0	7.10	414.0
0.0	10.10	413.8
0.0	12.10	412.8
0.0	16.10	414.7
0.02	4.40	407.1
0.02	10.10	405.0
0.02	13.10	405.3
0.02	15.90	405.2
0.04	11.93	395.6
0.04	14.10	394.7
0.04	16.60	393.9

^a The CO₂-free polymer weight fraction of all solutions amounts to 10 wt %.

solutions, two phenomena have to be taken into consideration:

(1) The hydrodynamic radii of hyperbranched polymers in solution predominantly depend on solvent properties such as pH and intrinsic viscosity.^{23,26}

(2) CO₂ represents an antisolvent for hydrophilic, aliphatic polymers and decreases the solvent power of polar solvents when added to the solution.

The addition of CO₂ to the aqueous polyester solution results in a sharp decrease in pH. In the presence of

Table 4. Partial Pressure Curve of Water for Gas-Free, Aqueous Hyperbranched Polyester Solutions (*w*_{polymer} = 0.10)

Boltorn H20–water		Boltorn H40–water	
<i>P</i> (MPa)	<i>T</i> (K)	<i>P</i> (MPa)	<i>T</i> (K)
0.045	348.2	0.046	350.6
0.052	353.7	0.062	358.4
0.069	361.2	0.073	363.1
0.083	366.5	0.087	368.2
0.095	370.1	0.107	374.0
0.113	375.5	0.123	378.2
0.135	381.0	0.145	383.1
0.163	386.6	0.185	390.9
0.203	393.4	0.271	403.3
0.235	398.3	0.320	408.8
0.291	405.4	0.363	413.2
0.346	411.4	0.418	418.2
0.387	415.4	0.477	423.2
		0.553	428.7
		0.622	433.4

CO₂, water becomes acidic due to the formation and dissociation of carbonic acid according to CO₂ + H₂O ↔ H₂CO₃ ↔ H⁺ + HCO₃[−]. Toews et al. showed²⁷ that the pH of water in equilibrium with supercritical CO₂ varies from 2.8 to 2.95 for 298 K < *T* < 343 K and 7 MPa < *P* < 20 MPa.⁴³

Investigations of a series of buffered aqueous Boltorn solutions (*w*_{polymer} = 0.10) have shown that, for pH ≤ 7, the cloud point temperature under saturation conditions (*T*^{LLV}) decreases with decreasing pH.²⁵ Therefore, it can be concluded that the addition of supercritical carbon dioxide to the Boltorn–water solutions (Figure 6 and Tables 3 and 4) decreases the pH successively, which, most likely, results in an increase of the hydrodynamic radii of the dissolved hyperbranched Boltorn H40 and Boltorn H20 macromolecules. Thus, at low pH, the hydroxyl groups of the hyperbranched polyesters are better accessible for the water molecules, leading to an increased polymer solubility and the corresponding shift of the respective UST curves to lower temperatures (see Figure 6).

It is worth mentioning that the comprehension of the phase behavior of dendritic polymer solutions is an essential prerequisite for contemporary polymer science and engineering. Phase separation and segregation often occur during the production and processing of polymers, either due to a process-based necessity or owing to undesirable circumstances such as the incompatibility between polymers or an insufficient solvent power. The results above have shown the pH-dependent solubility behavior of hyperbranched polyesters, i.e., coherences which, for instance, are important to ensure the homogeneity of a dendritic polymer solution. In this context it is noteworthy that the sales specifications of commercially available hyperbranched polymers sometimes do not guarantee a constant acidity/basicity, which might lead to a considerable change in the phase behavior if one uses the same kind of a hyperbranched polymer but from different batches.⁴⁴

3.2.2. Hyperbranched Polyester–Ethanol–CO₂

Figure 7 shows UST and LST curves of the system Boltorn H20–ethanol–CO₂. By comparing the UST curves of the gas-free hyperbranched polyester solutions of Figure 6 (Tables 3 and 4) and Figure 7 (Table 5), the increased Boltorn H20 solubility in ethanol becomes obvious. Furthermore, when adding CO₂ to the solution of 10 wt % of polymer, it can be seen that the locations of the UST curve do not depend on the CO₂ concentra-

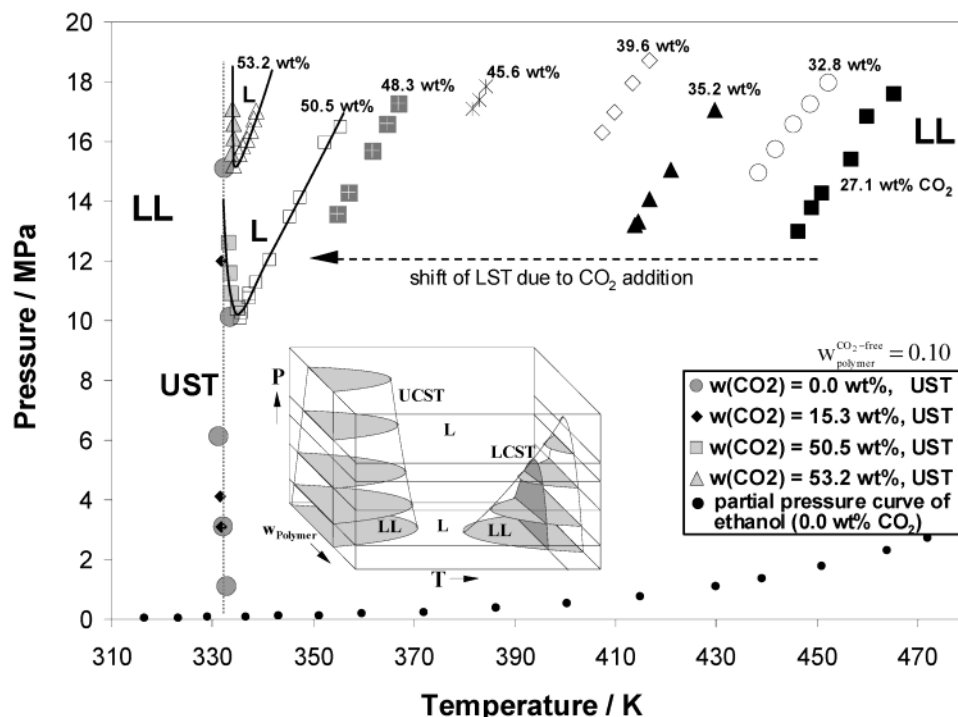


Figure 7. High-pressure phase behavior of the system hyperbranched polyester Boltorn H20-ethanol- CO_2 .

tion anymore. Since, for ethanol as solvent, no carbonic acid formation and no pH phenomenon can occur, the UST location of this solution does not change with increasing gas content even at large CO_2 concentrations ($w_{\text{CO}_2} = 15.3$ wt %). This result is in accordance to the demixing behavior of gas-expanded solutions containing linear polymers, such as previously observed for the system polystyrene-cyclohexane- CO_2 .²⁸ Unlike the enthalpic dominated liquid-liquid phase separation at moderate temperatures ($T \leq T_{\text{UCST}}$), at higher system temperatures the entropic contribution to the Gibbs free energy of the mixture g_{mix} dominates the enthalpic contribution, resulting in a negative second derivative of g_{mix} [$(\partial^2 g_{\text{mix}} / \partial x^2)_{T,P} < 0$] and thus the formation of another liquid-liquid miscibility gap at $T \geq T_{\text{LCST}}$.

The LCST curve of the CO_2 -free hyperbranched polyester-ethanol system is located in the temperature and pressure range, which—due to the design criteria of the autoclave (see section 2.1.2)—was not accessible. Therefore, CO_2 was added to a hyperbranched polyester-ethanol solution of $w_{\text{polymer}} = 0.10$, resulting in a decrease of the solvent power and the corresponding shift of the LST curve to lower temperatures. For the CO_2 concentration of $w_{\text{CO}_2} = 27.1$ wt %, the LST curve of the system entered the experimentally accessible pressure range (see Figure 7, Table 5). Unlike the UST curves, the cloud point temperatures of the LST curves crucially depend on the system pressure and the CO_2 concentration. Moreover, the higher the carbon dioxide concentration, the larger the size of the gas-expanded LCST miscibility gap and the smaller the homogeneous temperature corridor between the LST and UST curves. Eventually, at the CO_2 concentration of $w_{\text{CO}_2} = 50.5$ wt % the LST and the UST curve meet each other, resulting in the merging of the two miscibility gaps into one area of complete immiscibility, known as the hourglass.

Generally, hydroxyl-functional polymers show a complex competition between the highly oriented hydrogen-bonding forces, the dispersion forces, and the combina-

torial entropy of mixing. This competition, with its different contributions to the Helmholtz energy of mixing, can also lead to the closed loop behavior such as that observed for poly(vinyl alcohol) and poly(ethylene glycol) solutions.^{29,30} The phase behavior of the system Boltorn H20-ethanol- CO_2 corresponds to type IV of the classification of van Konynenburg and Scott.^{31,32} Nevertheless, further investigations are necessary to show how this type of phase behavior changes with the degree of polymer branching and the nature and number of polymer functionalities.

4. Conclusions and Future Work

An extensive experimental study on the phase behavior of hyperbranched polymer solutions has been presented. At moderate pressures the investigated VLE of commercially available hyperbranched polymers such as polyesters, polyesteramides and polyglycerols in ethanol or in water allowed for a discussion on how the nature and number of polymer functionalities, the degree of polymer branching and the solvent polarity determines the slope of the bubble point curve and the solvent activity. It was found that the VLE primarily depends on the interactions between the solvent molecules and the polymer functionalities. Neither the molecular structure nor the molecular weight of the investigated hyperbranched polymers changed the absorption behavior of the macromolecules considerably. At large polymer concentrations, due to the great number of functionalities, hydroxyl-functional hyperbranched polyesters tend to form agglomerates. This has to be taken into account when discussing the solubility of hydroxyl-functional hyperbranched polymers.

Furthermore, cloud point measurements of aqueous polyester solutions in the presence of supercritical carbon dioxide lead to the conclusion that the enthalpic-dominated phase behavior in the vicinity of the upper critical solution temperature strongly depends on the pH. This might be of great importance for the produc-

Table 5. UST and LST Results of the System Hyperbranched Polyester–Ethanol–CO₂^aBoltorn H20–Ethanol–CO₂

UST Measurements

w_{CO_2}	P (MPa)	T (K)	w_{CO_2}	P (MPa)	T (K)
0.0	1.10	332.9	0.0	15.10	332.4
0.0	3.10	332.1	0.153	3.10	331.8
0.0	6.10	331.2	0.153	4.10	331.5
0.0	10.10	333.5	0.153	12.00	331.6

UST/LST Merging

w_{CO_2}	P (MPa)	T (K)	w_{CO_2}	P (MPa)	T (K)
0.505	10.4	335.0	0.505	16.50	355.4
0.505	10.9	333.8	0.532	15.60	333.8
0.505	11.6	333.5	0.532	16.10	334.1
0.505	12.6	333.2	0.532	16.60	334.1
0.505	10.09	335.5	0.532	17.10	334.0
0.505	10.27	335.7	0.532	15.20	334.1
0.505	10.75	337.3	0.532	15.59	335.2
0.505	10.90	337.4	0.532	15.86	336.0
0.505	11.28	338.6	0.532	16.07	336.8
0.505	12.05	341.3	0.532	16.38	337.6
0.505	13.47	345.3	0.532	16.76	338.2
0.505	14.10	347.3	0.532	17.02	338.7
0.505	15.97	352.4			

LST Measurements

w_{CO_2}	P (MPa)	T (K)	w_{CO_2}	P (MPa)	T (K)
0.271	12.97	446.2	0.352	15.07	421.0
0.271	13.78	448.9	0.352	17.06	429.7
0.271	14.26	450.9	0.396	16.32	407.2
0.271	15.38	456.7	0.396	16.99	409.8
0.271	16.83	459.8	0.396	17.98	413.4
0.271	17.57	465.2	0.396	18.73	416.6
0.328	14.94	438.5	0.456	17.10	381.5
0.328	15.74	441.8	0.456	17.40	382.9
0.328	16.56	445.4	0.456	17.84	384.3
0.328	17.23	448.7	0.483	13.56	354.7
0.328	17.95	452.3	0.483	14.30	357.0
0.352	13.21	413.8	0.483	15.72	361.7
0.352	13.32	414.4	0.483	16.63	364.5
0.352	14.09	416.6	0.483	17.31	366.8

Partial Pressure Curve of Ethanol ($w_{\text{CO}_2} = 0.0$)

P (MPa)	T (K)	P (MPa)	T (K)
0.036	316.5	0.377	386.2
0.047	323.2	0.515	400.4
0.058	329.0	0.740	415.0
0.077	336.6	1.083	429.9
0.096	343.0	1.340	439.1
0.127	351.1	1.756	451.0
0.174	359.6	2.309	464.0
0.237	371.9	2.709	472.1

^a The CO₂-free polymer weight fraction of all solutions amounts to 10 wt %.

tion, processing, and appliance of hyperbranched polymers, since a slight change in the hydroxyl and/or acid number of a polymer could lead to a considerable change in the phase behavior. The high-pressure phase behavior of nonaqueous hyperbranched polyester solutions shows the characteristics of a type-IV system according to the classification of van Konynenburg and Scott. The location of the upper solution temperature curve proved to be dependent on the molecular polymer weight and the solvent polarity and independent of the system pressure. However, the slope of the lower solution temperature curve strongly depends on the pressure. Moreover, an increase in CO₂ concentration leads to a considerable shift of the lower solution temperature

curve to lower system temperatures. For the system hyperbranched polyester–ethanol–CO₂ the merging of the UST and the LST curve into the hourglass miscibility gap is observed at a CO₂ concentration of 50.5 wt %.

Future work will focus explicitly on the influence of polymer branching on the phase behavior of polymer solutions. High-pressure PVT data will be provided for a variety of hyperbranched polymers. Subsequently, the ability of thermodynamic models such as the perturbed-chain SAFT equation of state,³³ COSMO–RS,³⁴ or g^E models^{35–37} to describe enthalpic and entropic phenomena of the phase behavior of highly branched polymer solutions will be tested and possibly modified, so that the adequate consideration of the degree of polymer branching and the number and nature of polymer functionalities can be ensured.

Acknowledgment. The authors gratefully acknowledge the valuable contributions of Prof. John Prausnitz. We are indebted to him for guiding the development of our institute. This work was supported by the Deutsche Forschungsgemeinschaft under Grant Ar 236/2-4.

References and Notes

- (1) Geddes, R. In *The Polysaccharides*; Aspinall, G. O. Ed.; Academic Press: London and New York, 1985; Vol. 3, Glycogen: A Structural Viewpoint, p 209 and references therein.
- (2) Flory, P. J. *Principles of polymer chemistry*; Cornell University Press: Ithaca, NY, 1952.
- (3) Seiler, M. *Chem. Eng. Technol.* **2002**, 25, 237–253.
- (4) Seiler, M.; Köhler, D.; Arlt, W. *Sep. Purif. Technol.* **2003**, 30, 179–197.
- (5) Pirrung, F. O. H.; Loen, E. M.; Noordam, A. *Macromol. Symp.* **2002**, 187, 683–694.
- (6) Kim, Y. H.; Webster, O. W. *J. Am. Chem. Soc.* **1990**, 112, 4592–4593.
- (7) Frey, H.; Haag, R. *Mol. Biotechnol.* **2002**, 90, 257–268.
- (8) Seiler, M.; Suttirungwong, S.; Smirnova, I.; Arlt, W. *Polymer*, submitted for publication (and references therein).
- (9) Seiler, M.; Arlt, W.; Kautz, H.; Frey, H. *Fluid Phase Equilib.* **2002**, 201, 359–379.
- (10) Arlt, W.; Seiler, M.; Sadowski, G.; Frey, H.; Kautz, H. DE Pat. No 10160518.8, 2001.
- (11) Seiler, M.; Arlt, W.; Kavarnou, A.; Buggert, M.; Rolker, J.; Falah, M. Y.; Köhler, D. Lecture at the international Polydays conference, Berlin, 2002.
- (12) Tomalia, D. A.; Fréchet, J. M. J. *J. Polym. Sci., Part A: Polym. Chem.* **2002**, 40, 2719–2728.
- (13) Jikei, M.; Kakimoto, M. *Prog. Polym. Sci.* **2001**, 26, 1233–1285.
- (14) Inoue, K. *Prog. Polym. Sci.* **2000**, 25, 453–571.
- (15) Sadowski, G.; Mokrushina, L. V.; Arlt, W. *Fluid Phase Equilib.* **1997**, 139, 391–403.
- (16) Bungert, B.; Tippl, R.; Sadowski, G.; Arlt, W. In *High-Pressure Chemical Engineering*; van Rohr, P. R., Trepp, C., Eds.; Elsevier: Amsterdam, 1996; pp 519–524.
- (17) Bungert, B.; Sadowski, G.; Arlt, W. *Fluid Phase Equilib.* **1997**, 139, 349–359.
- (18) Chen, S.; Economou, I. G.; Radosz, M. *Fluid Phase Equilib.* **1993**, 83, 391–398.
- (19) van Vliet, R. E.; Dreischor, M. W.; Hoefsloot, H. C. J.; Iedema, P. D. *Fluid Phase Equilib.* **2002**, 201, 67–78.
- (20) Striolo, A.; Prausnitz, J. M. *Polymer* **2000**, 41, 1109–1117.
- (21) Jang, J. G.; Bae, Y. C. *Chem. Phys.* **2001**, 269, 285–294.
- (22) Striba, S. E.; Kautz, H.; Frey, H. *J. Am. Chem. Soc.* **2002**, 124, 9698–9699.
- (23) Xu, M.; Yan, X.; Cheng, R.; Yu, X. *Polym. Int.* **2001**, 1338–1345.
- (24) Prausnitz, J. M. Personal communication, 2002.
- (25) Seiler, M.; Arlt, W. Unpublished results, 2002.
- (26) Newkome, G. R.; Moorefield, C. N.; Baker, G. R.; Saunders, M. J.; Grossman, S. H. *Angew. Chem., Int. Ed. Engl.* **1991**, 30, 1178–1180.

- (27) Toews, K. L.; Shroll, R. M.; Wai, C. M.; Smart, N. G. *Anal. Chem.* **1995**, *67*, 4040–4043.
- (28) Bungert, B.; Sadowski, G.; Arlt, W. *Ind. Eng. Chem. Res.* **1998**, *37*, 3208–3220.
- (29) Rehage, G. *Kunststoffe* **1963**, *53*, 605–614.
- (30) Hino, T.; Lambert, S. M.; Soane, D. S.; Prausnitz, J. M. *AIChE J.* **1993**, *39*, 837–845.
- (31) Scott, R. L.; van Konynenburg, P. H. *Discuss. Faraday Soc.* **1970**, *49*, 87–97.
- (32) van Konynenburg, P. H.; Scott, R. L. *Philos. Trans. R. Soc. London Ser. A* **1980**, *298*, 495–540.
- (33) Gross, J. Entwicklung einer Zustandsgleichung für einfache, assoziierende und makromolekulare Stoffe. Dissertation, Technical University of Berlin, 2001.
- (34) Klamt, A.; Eckert, F. *Fluid Phase Equilib.* **2000**, *172*, 43–72.
- (35) Jang, J. G.; Huh, J. Y.; Bae, Y. C. *Fluid Phase Equilib.* **2001**, *194–197*, 675–688.
- (36) Kouskoumvekaki, I. A.; Giesen, R.; Michelsen, M. L.; Kontogeorgis, G. M. *Ind. Eng. Chem. Res.* **2002**, *41*, 4848–4853.
- (37) Panayiotou, C.; Missopolinou, D. *Fluid Phase Equilib.* **1999**, *156*, 51–56.
- (38) Seiler, M.; Buggert, M.; Kavarnou, A.; Arlt, W. *J. Chem. Eng. Data* **2002**, in press.
- (39) Seiler, M.; Arlt, W.; Kautz, H.; Frey, H. Unpublished results, 2002.
- (40) Currently Perstorp Speciality Chemicals AB, produces hyperbranched polymers, known as Boltorn products, on a ton-scale for 12 Euro/kg.
- (41) The results were presented by M. Seiler, J. Rolker, and W. Arlt at the 17th IUPAC Conference on Chemical Thermodynamics (ICCT), Rostock, Germany, 2002.
- (42) The linear polyglycerol ($M_n = 1400$ g/mol, Hyperpolymers GmbH) represents the perfect analogue to the hyperbranched polyglycerol ($M_n = 1400$ g/mol, Hyperpolymers GmbH), since both polymers only differ in the degree of branching but not in the molecular weight nor the number of hydroxyl groups. For further details concerning the synthesis and the properties of these differently branched polyglycerols, see the recent results of Frey and co-workers.²²
- (43) For instance, the pH of an aqueous CO₂ solution at 343 K changes from 2.95 to 2.84, when the pressure of the supercritical CO₂ increases from 7 to 20 MPa.²⁷
- (44) The hyperbranched Boltorn products of the Perstorp Group for instance show a varying hydroxyl and acid number (see Table 1), whose range has to be taken into account.

MA025994N